

1992

A global optimization algorithm for heat exchanger networks

Ignacio Quesada
Carnegie Mellon University

Ignacio E. Grossmann

Carnegie Mellon University. Engineering Design Research Center.

Follow this and additional works at: <http://repository.cmu.edu/cheme>

Published In

.

This Technical Report is brought to you for free and open access by the Carnegie Institute of Technology at Research Showcase @ CMU. It has been accepted for inclusion in Department of Chemical Engineering by an authorized administrator of Research Showcase @ CMU. For more information, please contact research-showcase@andrew.cmu.edu.

NOTICE WARNING CONCERNING COPYRIGHT RESTRICTIONS:

The copyright law of the United States (title 17, U.S. Code) governs the making of photocopies or other reproductions of copyrighted material. Any copying of this document without permission of its author may be prohibited by law.

**A Global Optimization Algorithm
for Heat Exchanger Networks**

I. Quesada, I.E. Grossmann

EDRC 06-138-92

A Global Optimization Algorithm for Heat Exchanger Networks

Ignacio Quesada and Ignacio E. Grossmann*
Department of Chemical Engineering
Carnegie Mellon University
Pittsburgh, PA 15213

May 1992

*** Author to whom correspondence should be addressed**

Abstract

This paper deals with the global optimization of heat exchanger networks with fixed topology. It is shown that if linear area cost functions are assumed, as well as arithmetic mean driving force temperature differences in networks with isothermal mixing, the corresponding NLP optimization problem involves linear constraints and linear rational functions in the objective which are nonconvex. A rigorous algorithm is proposed that is based on a convex NLP underestimator that involves linear and nonlinear estimators for rational and bilinear terms which provide a tight lower bound to the global optimum. This NLP problem is used within a spatial branch and bound method for which branching rules are given. Basic properties of the proposed method are presented, and its application is illustrated with several example problems. The results show that the proposed method only requires few nodes in the branch and bound search.

Mathematical model

Two major simplifications have been assumed in the optimization model of heat exchanger networks that provide a mathematical structure that can be exploited for the global optimization. The area cost is given by a linear function and the driving force for the heat exchangers is calculated by the arithmetic mean temperature difference at both ends of the heat exchanger.

For a given heat exchanger network (HEN) configuration consisting of n exchangers of which the subset EU are utilities, the mathematical formulation can be stated as a linearly constrained NLP problem of the following form:

$$\begin{aligned} \min C = & \sum_{i=1}^n \frac{q}{U_i} \frac{Q_i}{\Delta T_i} + \sum_{j \in EU} d_j Q_j \\ \text{s.t. } & g(Q, AT, x) \leq 0 \\ & X \in X \end{aligned} \quad (P)$$

$$Q_i^L \leq Q_i \leq Q_i^U, \Delta T_i \geq \Delta T_i^{\text{SAT}} \quad i=1, \dots, n$$

where Q_i corresponds to the heat load of the heat exchanger i and ΔT_i is the driving force for the heat exchanger; H_i is the heat transfer coefficient, q is the area cost coefficient and d_j^* the utility cost. The lower bounds for the driving forces, ΔT_i^L , are strictly positive since fixed network configurations are considered and they have to be greater or equal than a minimum exchanger approach temperature, EMAT. The heat loads Q_i are nonnegative, although valid finite lower and upper bounds as is the case for ΔT_i can be obtained by preanalysis of a given network structure. The variables x are all the additional variables in the formulation (i.e. intermediate temperatures). The function g involves a set of linear constraints that describe networks that can be embedded in the superstructure of Yee and Grossmann (1991) in which isothermal mixing of streams is assumed. These constraints include heat balances, definition of driving forces and approach temperature constraints. An example of problem (P) is given later in the paper (model (PEX)).

The difficulty in solving problem (P) lies in the fact that it has a nonconvex objective function that can have multiple local minima. Furthermore, these local solutions will not necessarily correspond to extreme points of the feasible region since the objective function is the sum of linear fractional functions. Each of these functions is pseudolinear (pseudoconvex and pseudoconcave), **which means that they can project** either as monotonically **increasing or** monotonically **decreasing functions**. **In this way the complete objective function is neither** convex nor concave **and the local solutions can be extreme or non extreme points** (

Motivating Example

Consider the HEN illustrated in Figure 1. This network has four heat exchangers and consists of one cold stream, C1, which is split and directed into exchangers 1 and 2. The two hot streams, H1 and H2, exchange heat in series with cold streams C2 and C1, and C3 and C1, respectively. The inlet and outlet temperatures and the heat capacity flowrates are given in Table 1. Note that the outlet temperatures for the cold streams C2 and C3 are not specified. The objective in this problem is the minimization of the cost of the total area C in which the cost coefficients are $c_1 = 2,700 \$/m^2$, $c_2 = 7,200 \$/m^2$, $c_3 = 2,400 \$/m^2$ and $c_4 = 9,000 \$/m^2$ and the overall heat transfer coefficients are $U_1 = U_2 = 0.1 \text{ kW/Km}^2$ and $U_3 = U_4 = 1 \text{ kW/Km}^2$.

Based on model (P), the mathematical formulation for minimizing the cost in this network is given by:

$$\begin{aligned} \min C &= 2700 \frac{Q_1}{0.1 \Delta T_1} + 7200 \frac{Q_2}{0.1 \Delta T_2} + 2400 \frac{Q_3}{\Delta T_3} + 9000 \frac{Q_4}{\Delta T_4} \\ \text{st. } Q_1 &= 5.55 (T_1 - 395) \\ Q_2 &= 3.125 (T_2 - 362.5) & \text{(PEX)} \\ Q_3 &= 4.54 (T_3 - 370) \\ Q_4 &= 5.55 (580 - T_4) \\ Q_4 &= 3.571 (T_4 - 352.5) \\ Q_4 &= 3.125 (512.5 - T_2) \end{aligned}$$

$$T_j > 400 + 5$$

$$T_3 > 400 + 5$$

$$Q_i + 0.2 = 100$$

$$\Delta T_1 = \frac{T_i - 305}{2}$$

$$\Delta T_2 = \frac{T_2 - 302}{2}$$

$$\Delta T_3 = \frac{T_1 - T_3 + 210}{5}$$

$$\Delta T_4 = \frac{T_2 - T_4 + 360}{5}$$

$$395 < T_1 < 575$$

$$398 < T_2 < 718$$

$$365 < T_3$$

$$358 < T_4$$

$$Q_i \geq 0, \Delta T_i \geq 10, i=1, \dots, 4$$

in which a value of EMAT = 5 (minimum exchanger approach temperature) has been assumed. Since the problem has a total of 12 variables and 11 independent equations it has one degree of freedom. Figure 2 shows the objective function of this formulation, the total area cost of the network, plotted against Q_i , the heat load of the first heat exchanger. The feasible region for the network, $Q_i \in [5.55, 97.81]$, is defined by the minimum approach temperature constraints. As it can be seen in Fig. 2 there are two local optimal solutions. The first local solution with cost O\$ 45,687 is located in the convex portion of the projection of the objective function and it corresponds to the interior point $Q_i = 16.84$ kW with a total area of 9.351 m^2 . The second local solution with cost $C = \$36,160$ corresponds to the global optimum. It lies at an extreme point in the concave part and is defined by the approach temperature constraint of heat exchanger 2; it is located at $Q_i = 97.812$ kW with a total area of 9.254 m^2 . When a local search technique is used for solving this problem, the solution will depend of the initial point that is given. The next sections will develop a solution method that will rigorously determine the global optimum for this problem regardless of the initial point that is selected.

Underestimator and overestimator functions

Problem (P) can be reformulated by introducing the variables A for the scaled areas (the product of the area and the overall heat transfer coefficient) of the exchangers, and extra constraints to relate each of these to its heat load and driving force. This yields the following problem formulation.

$$\begin{aligned} \min C &= \sum_{i=1}^n \frac{Q_i}{U_i} A_i + \sum_{i \in EU} d_i Q_i \\ \text{st. } A_i \Delta T_i - Q_i &\geq 0, & i=1, \dots, n \\ g(Q, \Delta T, x) &\leq 0 & \text{(PI)} \\ x &\in X \\ (Q_i, \Delta T_i, A_i) &\in A_i \end{aligned}$$

$$\text{where } A_i = \{Q_i^L \leq Q_i \leq Q_i^U, \Delta T_i^L \leq \Delta T_i \leq \Delta T_i^U, A_i^L \leq A_i \leq A_i^U\}, \quad i=1, \dots, n$$

In problem (P) the nonconvexities appear in the form of bilinear terms in the constraints. In order to develop a valid lower bound to the global optimum, the nonconvex terms in (PI) can be replaced by the linear overestimating functions proposed by McCormick (1983) (see Appendix A eq A4). These functions can be expressed by the set of two inequalities for each exchanger $i=1, \dots, n$,

$$A \Delta T_i \leq A^L \Delta T_i + A \Delta T_i^U - A^L \Delta T_i^U \quad (1)$$

$$A \Delta T_i \geq A^U \Delta T_i - A \Delta T_i^L + A^U \Delta T_i^L \quad (2)$$

The above inequalities can be used to replace the bilinear terms in (PI) yielding an LP underestimator problem. However, the predicted bounds by this problem are often not very tight. For this reason a new set of nonlinear convex underestimator functions are proposed that can be generated from the original formulation (P) over the linear fractional terms of the objective function (see Appendix A eq A14). Expressing the proposed nonlinear underestimators in the form of inequalities yields:

$$\frac{Q_i}{A_i} \geq A_i^{u+win} A_i^L, \quad A_i^U \quad (3)$$

$$\frac{Q_i}{\Delta T_i} \geq \frac{Q_i}{\Delta T_i^L} + Q_i^U \left(\frac{1}{\Delta T_i} - \frac{1}{\Delta T_i^L} \right) \quad (5)$$

The following mathematical properties can be established between the linear and nonlinear estimator functions in (1) and (2) and (3) and (4).

Property-1: When A^{QL} (or A^{QU}) the linear overestimator (1) (or (2)) is a linearization of the nonlinear underestimator (3) (or (4)).

Proof Consider the linear overestimator (1) and the area constraint form (PI),

$$A_i \geq \frac{Q_i}{\Delta T_i} + A_i^L \Delta T_i \quad (5)$$

Rearranging (5) leads to:

$$A_i \geq \frac{Q_i}{\Delta T_i^U} - \frac{A_i^L \Delta T_i}{\Delta T_i^U} + A_i^L \quad (6)$$

Using the condition that $A_i^L \Delta T_i > 0$, equation (6) yields

$$A_i \geq \frac{Q_i}{\Delta T_i^U} - \frac{Q_i^L \Delta T_i}{(\Delta T_i^U)^2} + \frac{Q_i^L}{\Delta T_i^U} \quad (7)$$

The nonlinear underestimator (3) gives rise to the constraint

$$A_i \geq \frac{Q_i}{\Delta T_i^U} + Q_i^L \left(\frac{1}{\Delta T_i} - \frac{1}{\Delta T_i^U} \right) \quad (8)$$

The first term of equations (7) and (8) are the same. Now compare the term $\frac{1}{\Delta T_i} - \frac{1}{\Delta T_i^U}$ from the nonlinear underestimator (8) with the term $\frac{1}{\Delta T_i^U} - \frac{A_i^L \Delta T_i}{(\Delta T_i^U)^2}$ from the linear equation (7).

Both terms are equal at ΔT_i^U . Furthermore, a linearization of the nonlinear term of (8) at ΔT_i^U yields the linear term:

$$-\frac{1}{(\Delta T_i^U)^2} \Delta T_i \quad \frac{1}{\Delta T_i^U} - \frac{A_i^L \Delta T_i}{(\Delta T_i^U)^2}$$

Thus, (3) is a linearization of (1) ■

Corollary 1. The nonlinear underestimator (3) (or (4)) is stronger than the linear overestimator

(1) (or (2)) when $A^{\wedge j}$ (or $A^u = \frac{Q^u}{\Delta T_1^L}$).

Proof. From Property 1 and the fact that the nonlinear underestimators in (3) and (4) are convex in AT_f any linearization is smaller or equal than the function (see Fig. 3).

The following property, however, establishes that the linear overestimators in (1) and (2) are not necessarily redundant

Property 2. When $A^L > \frac{Q^L}{\Delta T_1^J}$ (or $A^{\wedge} < \frac{Q^u}{\Delta T_1^c}$) there is a part of the feasible region in which the linear overestimator (1) (or (2)) is stronger than the nonlinear underestimator (3) (or (4)).

Proof. Consider a feasible point in A , such that $A^{\wedge} = A^{\wedge}$. with $Q_i^* > Q_t^L$ and $AT_i^* < T_1^u$.

Evaluating the linear overestimator (1) at (Q_r^+, AT_1^+) yields:

$$A_1 \geq \frac{Q^+}{\Delta T_1^u} - \frac{A^L \Delta T_1^+}{\Delta T_1^u} + A_1^L = \frac{A^L \Delta T_1^+}{\Delta T_1^u} - \frac{A^L \Delta T_1^+}{\Delta T_1^u} + \quad (10)$$

Then the linear overestimator for that point reduces to,

$$A_1 \geq A^L \quad (11)$$

The nonlinear underestimator (3) for this point is,

$$A_1 \geq \frac{Q^+}{\Delta T_1^u} + Q^+ \left(\frac{1}{\Delta T_1^+} - \frac{1}{\Delta T_1^u} \right) \quad (12)$$

and using the relation $A^{\wedge} = A^L$ for expressing (12) in terms of A^{\wedge} yields.

$$A_1 \geq \left[\frac{\Delta T_1^+}{\Delta T_1^u} + \frac{Q^+}{Q^r} \right] A^L - \frac{Q^+}{\Delta T_1^u} \quad (13)$$

Define $\alpha = \frac{\Delta T_1^+}{\Delta T_1^u}$ and $\beta = \frac{Q^+}{Q^r}$. the equation (13) can be expressed as.

$$A_1 \geq [\alpha + \beta] A^L - \alpha \beta A^L = A^L [\alpha + \beta (1 - \alpha)] \quad (14)$$

Since $0 < \alpha < 1$ and $0 < \beta < 1$

$$1 = \alpha + (1 - \alpha) > \alpha + \beta(1 - \alpha) = \quad (15)$$

then the nonlinear underestimator reduces to

$$A_t \geq \phi A_t^L, \quad \phi < 1 \quad (16)$$

Hence, the linear overestimator (1) is stronger at the point (Q_t, AT^u) .

B

In a similar way that nonlinear underestimator functions are used to obtain a convex approximation for the terms $A_j = \frac{Q}{T}$, underestimating functions can be generated for the terms $AT_t > \hat{}$,

$$\frac{Q_t}{A_t} \geq \frac{Q_t}{A_t^U} + Q < \hat{} \quad ,17,$$

$$\frac{Q_t}{A_t} \geq \frac{Q_t}{A_t^L} + Q^{U^*} \left(\frac{1}{A_t} - \frac{1}{A_t^L} \right) \quad (18)$$

However, In this case the limitation is that (17) and (18) are only defined for the case when the lower bound A_f is greater than zero.

Geometrical Interpretation

The underestimator and overestimator functions (1) - (4) presented In the previous section have the property that they match exactly the original function at the boundary of the feasible region A_x of problem (PI) (see Appendix B for a proof). The fact that these estimator functions are nonredundant over the feasible region can be interpreted geometrically in a 2-dimensional diagram (see Figure 4). For a particular heat exchanger It Is possible to represent its feasible region A_t in a 2-dimensional figure by plotting its driving force versus its heat load. In this diagram the area of the heat exchanger Is given by the straight lines that pass through the origin and have a positive slope. The nonlinear underestimators (3) and (4) provide an exact approximation along the boundaries defined by the lower and upper bounds for the heat load, Q , and the driving force, AT . The linear underestimators (1) and (2) provide an exact approximation at the lower and upper bounds for the area. A , and the driving force, AT . In the case that $A^L = \frac{Q_L}{T^L}$ (or $A^u = \frac{Q_U}{T^U}$) the line that defines this boundary does not cut any part of the feasible region that Is already defined by the bounds of the heat load and the driving force resulting In a redundant linear overestimator. When this is not the case, then there exists a part of the feasible region in which the bound of the area Is stronger than the boundaries

determined by the bounds of the heat load and driving force (see Fig. 4). At these boundaries (A^L, A^u), the linear overestimators provide an exact representation of the original functions while the nonlinear underestimators give a weaker approximation. In this way both estimators complement each other in the approximation of the fractional terms.

Bounds.

Valid lower and upper bounds of the area, driving force and heat load of each heat exchanger (A_i, AT_i, Q_i) are required for the under and overestimator functions in (1) - (4). These bounds can be specified by nonnegativity conditions and approach temperatures specifications. However, in order to take advantage of the fact that the feasible region of problem (PI) is **convex and** described by a set of **linear constraints**, one can explicitly obtain the **strongest bounds possible** since these are the ones that determine the tightness of the approximation functions.

For generating the strongest upper and lower bounds it is necessary to solve a sequence of LP's in which the objective function is either min (or max) AT_i , or min (or max) Q_i over the set of linear constraints. In the case of the bounds for the areas the objective function is min (or max) A_i . This corresponds to a linear fractional programming problem that is equivalent to an LP by using the transformation proposed by Charaes & Cooper (1962). The LP problems for determining variable bounds have the same feasible region and are Independent, so they can be easily updated or solved in parallel.

From the bounds It is also possible to know in advance if some of the approximating functions are redundant. Based on Property 1, if $A^u = T^T$ (or if $A^L = -SJJ$) then the linear overestimator (2) that involves A^u (or A^L) will be redundant.

Projections

Since the linear fractional terms in problem (P) are pseudolinear they can give rise to monotonically increasing (convex) or monotonically decreasing (concave) directions in the feasible region. The convex envelope of a concave function is the straight line between the

extreme points. In the case of a convex function, its convex envelope is the function itself. In the 2-dimensional diagram of the feasible region of a particular heat exchanger, there are both concave and convex directions of the fractional term defining the area of that heat exchanger. It is easy to show that the straight lines with positive slope represent the concave directions, while the straight lines with a negative slope correspond to the convex directions (see Fig. 5). Specifically, let

$$AT_j = a + bQ_i \quad (19)$$

Then for $AT \leq \frac{Q}{\Delta T_1}$

$$A_i \geq \frac{Q}{a+bQ_i} \quad (20)$$

the right hand side of (20) has a positive second derivative for $b < 0$ (see also Property 3 later in this paper).

Since the nonlinear underestimator and linear overestimator functions (1)-(4) do not provide exact approximations in convex directions such as the ones shown in Fig 5, It is possible to develop exact nonlinear underestimators in the convex directions. These are obtained by expressing the lower and/or upper bounds of one variable as a function of the other variable involved in the estimator. In this case it is necessary to ensure that this nonlinear functionality does not destroy the convexity of the approximating function*

The proposed underestimator described above corresponds to a projection along the convex direction. As shown below, this projection can be obtained without any extra cost when bounds are generated for the variables in the approximating functions since the Lagrange multipliers of the bounding subproblems can be used to generate this projection.

Consider the case that the upper bound (equivalent for the lower bound) of the driving force AT , of a given heat exchanger is projected over its respective heat load Q_i (in a similar way projections can be obtained for the heat load over its driving force).

$$\begin{aligned} \min \quad & -AT_i \\ \text{st. } & g(Q_i, \Delta T_i) \leq 0 \end{aligned} \tag{P2}$$

A Benders cut for problem (P2) is given by:

$$-AT_i \geq -AT_i + \sum_j \lambda_j g_j(Q_i, \Delta T_i, x^*) \tag{21}$$

where λ_j are the Lagrange multipliers and x^* is the solution of all the remaining variables in the LP problem in (P2). The above projection results in.

$$0 \geq \sum_j \lambda_j g_j(Q_i, \Delta T_i, x^*) \tag{22}$$

This is a linear function that can be expressed as,

$$AT_i \leq a + bQ_i \tag{23}$$

This function has to have a negative slope ($b < 0$) to represent a convex direction of the objective function as was shown previously*. Therefore, it is possible to generate an additional convex nonlinear underestimator that is nonredundant to the previous ones (see Property 3), and it is given by:

$$AT_i \leq \frac{1}{a + bQ_i} \tag{24}$$

Property 3 The nonlinear inequality (24) is a valid convex underestimator when $b < 0$, and in some part of the feasible region A, is stronger than the nonlinear underestimators (3) and (4),

For the first part of the proof the constraint (23) can be expressed as:

$$\frac{1}{AT_i} \geq \frac{1}{a + bQ_i} \tag{25}$$

Multiplying by the lower bound constraint for the heat load ($Q_i \geq Q_i^{\min}$) yields a the valid inequalities:

$$Q_i - Q_i^{\min} \left(\frac{1}{AT_i} - \frac{1}{a + bQ_i} \right) \geq 0 \tag{26}$$

Rearranging yields:

$$\frac{Q}{\Delta T_1} \geq \frac{Q^L}{\Delta T_1} + (Q - Q^L) \left(\frac{1}{a + b Q} \right) \quad (27)$$

which correspond to the nonlinear underestimator (24).

The Hessian matrix of the underestimating function in (24) is given by

$$\begin{bmatrix} -\frac{2b(a+bQ^L)}{(a+bQ)^3} & 0 \\ 0 & \frac{2Q^L}{AT^3} \end{bmatrix} \quad (28)$$

The term $(a+bQ)$ is positive over all the feasible region since,

$$a+bQ, \text{ \& } AT, > EMAT > 0 \quad (29)$$

Also $Q, \text{ \& } 0$, and therefore.

$$\frac{2Q^L}{\Delta T_1^3} > 0 \quad (Q^L > 0 \text{ if not the function reduces to just one convex term}) \quad (30)$$

and

$$-\frac{2b(a+bQ^L)}{(a+bQ)^3} > 0 \text{ if } b < 0 \quad (31)$$

Therefore, if $b < 0$ the Hessian matrix is positive definite and the function is convex.

Now consider a feasible point in the strict interior in A , such that $AT^* = a + bQ$, and $AT^* < AT^U$. Equation (24) for the nonlinear underestimator with projection reduces to.

$$\frac{Q}{\Delta T_1^*} + Q^L \left(\frac{1}{\Delta T_1^*} - \frac{1}{\Delta T_1^*} \right) = \frac{Q}{\Delta T_1^*} \quad (32)$$

and therefore is an exact approximation of the linear fractional term in (24). Since AT^+ does not lie in the boundary of A , the nonlinear underestimator (3) yields.

$$\frac{Q^L}{\Delta T_1^*} + \frac{Q - Q^L}{AT^U} < \frac{Q^L}{\Delta T_1^*} + \frac{Q - Q^L}{\Delta T_1^*} \leq \frac{Q}{\Delta T_1^*} \quad (33)$$

which is a strict inequality. Thus the underestimator (24) is stronger than the nonlinear underestimator (3) in some part of the interior feasible region.

For the other underestimator (4) consider now a point such that $Q^+ = (AT - a)/b$ and $Q^f < Q^u$, such a point exists since the projections are nonredundant constraints.

Equation (24) for the nonlinear underestimator with projection reduces to,

$$\frac{Q^*}{a+bQ^*} \left(\frac{1}{AT} - \frac{1}{a+bQ^*} \right) = \frac{Q^*}{a+bQ^+} = \frac{Q^*}{AT}, \quad (34)$$

which is an exact approximation of the fractional term. The nonlinear underestimator (4) yields,

$$\frac{Q^*}{\Delta T_f^L} - \frac{1}{\Delta T_f^L} < \frac{1}{\Delta T_f^L} - \frac{1}{\Delta T_f^L} \quad (35)$$

which is an strict inequality.

Hence, there are parts of the feasible region where the projected underestimator (24) is stronger than the nonlinear underestimator (4).

It can happen that when the projection in (24) is obtained using the LP solution of problem (P2), only a simple bound over the variable is obtained (i.e. $b=0$; $a = AT$) instead of a linear inequality. In this case it is possible to solve an additional problem fixing the projection variable at a fixed value within the bounds (i.e. $Q = Q^f$ with $Q^L < Q^f < Q^u$).

The projected nonlinear underestimators in (24) are clearly useful when the feasible region of a given heat exchanger has interior faces with convex directions, since it is possible to obtain exact approximations of this exchanger at these faces. The usefulness of these underestimators will be shown with example 3 later in the paper.

In a similar way, projection terms can be generated for the lower bound of the driving force with respect to its driving force and substituted in (4),

$$\frac{Q_i}{AT} * \frac{Q_i}{a' + b'Q_i} + g_i U \left(\frac{1}{AT} - \frac{1}{a' + b'Q_i} \right) \quad (36)$$

where $a' + b'Q_i \geq AT$.

The projections that can be obtained for the bounds of the heat load in terms of its driving forces are reduced to the same ones.

Convex nonlinear underestimator problem

Having derived a number of linear and nonlinear bounding approximations for the bilinear and rational terms in (P) and (PI), a convex nonlinear underestimator problem (NLPJ for problem (P) can be defined as follows. Valid bounds over the areas, driving forces and heat loads are generated to define the set $Q = uA_{it} \quad i=1..oi$, and the nonconvexities of the original problem are substituted by the convex approximating functions (1) - (4). (17), (18), (24) and (36).

The projections for the upper and lower bounds of the driving forces over its heat load are given by functions $\langle KQ \rangle = a + bQ_i$ where the conditions of Property 3 are satisfied. The form of the underestimator problem NLP_L is the following:

$$\begin{aligned} \min C_L &= \sum_1^n c_i A_i + \sum_{i \in EU} d_i Q_i \\ \text{st. } A_i &\geq \frac{Q_i}{\Delta T_i^U} + Q_i^L \left(\frac{1}{\Delta T_i} - \frac{1}{\Delta T_i^U} \right) \\ A_i &\geq \frac{Q_i}{\Delta T_i^L} + Q_i^U \left(\frac{1}{\Delta T_i} - \frac{1}{\Delta T_i^L} \right) && \text{(NLPJ)} \\ Q_i &\leq A_i \Delta T_i + A_i \Delta T_i^U - A_i \Delta T_i^L && i=1..n \\ Q_i &\leq A_i \Delta T_i + A_i \Delta T_i^L - A_i \Delta T_i^U \\ \Delta T_i &\geq \frac{Q_i}{A_i^U} + Q_i^L \left(\frac{1}{A_i} - \frac{1}{A_i^U} \right) && i=1..n \text{ and } A_i^L > 0 \\ \Delta T_i &\geq \frac{Q_i}{A_i^L} + Q_i^U \left(\frac{1}{A_i} - \frac{1}{A_i^L} \right) \\ A_i &\geq \frac{Q_i}{WQ_i^L} + Q_i^L \left(\frac{1}{\Delta T_i} - \frac{1}{\phi^U(Q_i)} \right) && i=1..n \text{ for which } \phi^U \text{ is a linear} \\ A_i &\geq \frac{Q_i}{\phi^L(Q_i)} + Q_i^U \left(\frac{1}{\Delta T_i} - \frac{1}{\phi^L(Q_i)} \right) && \text{of } 0, \text{ with negative slope} \\ g(Q, \Delta T, x) &\leq 0 \end{aligned}$$

$x \in X$

$(Q, AT, A) \in I$

Property 4. Any feasible point (Q, AT, A, x) in problem NLP_L provides a valid lower bound to the objective function of problem (PI). Furthermore, the optimal solution C_L^* of (NLP_L) provides a valid lower bound to the global optimum (C^f) of problem (PI).

Proof. Any feasible point (Q, AT, A, x) for problem (NLP_L) is also a feasible solution to problem (P) since the inequalities $g(Q, AT, x) \leq 0$ are satisfied in both problems. Since the approximating functions in (NLP_L) represent a relaxation of the bilinear Inequalities in (PI), they have the effect of underestimating the objective function C of problem (PI). Thus it follows that at the given feasible point $C_L \leq C$.

For the global optimum (Q^*, AT^*, A^*, x^*) of problem (PI) it then follows that $C^f \leq C_L^*$ where C_L^* is the objective of NLP_L evaluated at that point. Since C_L^* is the optimal solution of NLP_L is unique due to its convexity. $C^f \leq C_L^*$ and thus $C \leq C_L^*$.

Corollary 2. If the optimum solution C_L^* from NLP_L is equal to the objective function value C^f from (PI) it corresponds to the global optimum of (PI).

Proof. If C is not the global optimal solution of problem (PI) then there exists a solution $C^* < C$. But by Property 4, $C^* \leq C_L^*$ which contradicts the assumption that $C < C_L^*$ is a solution to NLP_L .

■

Partitioning Scheme (with a lower bound)

Problem NLP_L will in general provide a tight lower bound to the original problem (PI). However, since there will often be a gap between the lower bound C_L from NLP_L and the actual objective function C , a spatial branch and bound search will be required to find the global optimal solution. Corollary 2 provides a termination criteria to this search. In this section an algorithm is presented that employs a partitioning scheme of the feasible region for the branch and bound search.

During this search procedure, valid lower bounds C^k over subregions Q^k and upper bounds C^u of the global solution are generated. The lower bounds are provided by the solution of convex underestimator problems NLP_L over given subregions Q^k of the feasible space (Property 4). Each subregion Q^k is defined by a set of lower and upper bounds of the area, heat load and driving force of the heat exchangers.

Any feasible solution of the set of original linear constraints clearly provides a valid upper bound to the global solution of problem (P). Feasible solutions are obtained when the bounds for the variables are calculated. Additionally the solution of the convex NLP underestimator problem is a feasible solution. For all these points only an evaluation of the original objective function is necessary to determine an upper bound. The best upper bound C^u is stored as the incumbent solution C^* .

In some cases, it may prove to be useful to solve the original nonconvex problem (P) with a given set of bounds (Q^k) and a particular initial point (a solution of a convex underestimator problem). This is mainly used in the case that the difference between the convex underestimator C_L^k and the incumbent solution C^* is small and the nonconvex problem can help in adjusting the value of the variables, particularly if the objective function has only small variations between local solutions.

When the lower bound C_L^k of a particular subregion is greater or equal that the incumbent solution C^* it is an indication that no further examination of this subregion is required. If a gap exists between the lower and upper bounds, the subregion Q^k is divided into smaller subregions Q^{k+1} and Q^{k+2} . so it is possible to have tighter convex underestimator problems. To divide the subregions it is necessary to select the nonconvex term corresponding to a heat exchanger j over which the partition of the feasible region is made. This selection rule is based on the largest weighted difference between the exact value of the nonconvex term in (P) and the convex approximation obtained by the solution of the convex underestimator problem (see also Al-Khayyal and Falk (1983), Sherali and Alameddine (1990)). This rule is given by:

Rule 1.

Determine $j \in \arg \max_i [q_i (\frac{Q_i}{\Delta T_i} - A_j)]$ as the nonconvex term over which partitioning is to be performed.

The motivation for this criterion is to select the term for which the difference in the approximation affects the most the value of the objective function, so that the existent gap can be reduced by partitioning its corresponding region A_j .

A second selection rule, that is a variation of Rule 1, can be considered. In this rule a parameter $\delta \in (0,1]$ is included and it defines an interval over which some candidate heat exchangers are considered.

Rule 2

Apply Rule 1 and set $U_j = c_j (\frac{Q_j}{\Delta T_j} - A_j)$

Define I^k for $c_j (\frac{Q_j}{\Delta T_j} - A_j) \geq \delta U_j$

Select $j \in I^k$ as the nonconvex term over which partitioning is to be performed.

When $\delta=1$ this selection rule reduces to Rule 1. When $\delta < 1$, a heat exchanger that has not been previously used is selected. The advantage of this rule is that exchangers that have not been previously selected can be partitioned and this allows for a tightening of their bounds as it will be discussed later.

Once that the j th heat exchanger has been selected it is necessary to decide over which variable A_j , Q_j or ΔT_j , the partitioning should be performed. It is possible to restrict the algorithm to make partitions exclusively over the space of the areas, heat loads or driving forces* although a combination of these may prove more useful. This aspect depends on how interdependent are the bounds of the variables with respect to the partition variable. Once that the variable bounds that define the partition of the feasible region are selected, an update in the bounds of the other variables of that particular heat exchanger is done for each of the new

subregions. For these bounding problems the partition constraints that defined the subregion are added to the linear constraints to provide tighter approximations.

In this work, the variable that is normally chosen for the partitions is the area A_j . In case that exchanger j has been previously selected it is convenient to check if the bounds of the driving force, AT_j , and the heat load, Q_j were updated. If there was a change in these bounds then the partition variable can remain the same. But if the bounds of a variable did not change, then it is more efficient to choose it as the partition variable in this iteration. Also, in cases where the bounds for the areas indicate that the linear overestimators are redundant it is better to select the heat load or driving force over the area as the partition variable.

The value of the variable at which the partition is made correspond to the one of the incumbent solution. Two subregions are created by the addition of the constraints:

$$\text{Either } z \leq z^* \text{ or } z \geq z^* \quad (37)$$

where z is either A_j , AT_j or Q_j depending on which variable was selected.

The partition scheme is illustrated in Fig. 6. The divisions over the heat load and the driving force correspond to rectangular partitions. The divisions over the area are partitions of the feasible region in the nonconvex direction of the linear fractional term.

It can happen that the value of the partition variable in the incumbent solution is at one of its bounds*. In this situations a different variable of the exchanger j is considered as the partition variable. If no variable (A_j , AT_j and Q_j) has a incumbent value that is not at a bound then a different exchanger is selected for partition. When no variable can be selected for the exchangers that do not have an exact approximation, then the value of the variables at the solution of the convex subproblem is used for the partition constraints.

Algorithm

The subregion k is defined by the sets of bounds for each exchanger (A^k) which are stored in ft^k . The solutions of the convex NLP underestimators are referred as (C_L^k) and the incumbent solution as 0 . The candidate subregions that require further examination are stored in the set F .

Step 0. Initialization.

Set $C^* = \infty$, $F = \emptyset$, select tolerances ϵ and γ

For each heat exchanger $i=1, \dots, n$ generate

-lower and upper bounds for the area, heat load and driving force ($A_i^L, A_i^U, Q_i, Q_i^L, Q_i^U, AT_i^L, AT_i^U$), $i=1, \dots, n$ by solving a sequence of linear programs similar to (P2).

-Optional: obtain projections of the variables (Le. as in (22)) using either the solutions of the previous bounding problems or problems at a fixed level for the projection variable

-Evaluate the original objective function for each of these feasible solutions. If $C < C^*$ set $C^* = C$ and store the solution as the incumbent solution f .

Store the bounds in ft^0 , and set $F = F \cup \{0\}$

Step 1. Convex underestimator problem

-Solve problem NLP_L for Q^0 to obtain Q^0 .

-Evaluate the original objective function C^0 . If $C^0 < C^*$ set $C^* = C^0$ and store the solution as the Incumbent solution 0 .

Step 2. Convergence

-For the subregions $j \in F$, If $C_L^j - C^* \leq \epsilon$ delete subregion J from F ($F = F \setminus \{J\}$)

-If $F = \emptyset$ the global solution is given by the Incumbent solution.

Step 3. Partition

-Take the last region $k \in F$ and apply the selection rule (Rule 1 or Rule 2) and choose the partition constraint (37)

-Subdivide subregion Q^k in subregions Q^{k+1} and Cl^{k+2} by adding the respective bound or inequality. Delete subregion Q^k from F and store subregions Q^{k+1} and ft^{k+2} in F ($F=(F\setminus\{k\}) \cup \{k+1,k+2\}$)

-Update the bounds in subregions $k+1$ and $k+2$ for the exchanger selected for the partition.

Step 4. Convex underestimator problems

-Solve problem NLP_L for ft^{k+1} and Q^{k*2} to obtain C_L^{k+1} and C_L^{k+2} .

-Evaluate the original objective function for each of these feasible solutions. If $C < C^*$ set $C^* = C$ and store the solution as the incumbent solution f).

-Optional: When the difference between the objective function of the convex underestimator problem NLP_L and the incumbent solution C^* is smaller than a given tolerance ($(C^* - C)/C^* < \epsilon$). solve the original nonconvex problem (P) for Q^{k+1} and/or Q^{k*2} using its convex solution as the initial point If $C < C^\#$ set $C^* = C$ and store the solution as the incumbent solution (*)

-If $C_L^{k+1} < C_L^{k+2}$ invert Cl^{k+1} and Q^{k*2} in F .

-go to step 2

Convergence

As for the convergence of the algorithm, it should be noted that Al-Khayyal and Falk (1983) and Sherali and Alameddine (1990) presented branch and bound algorithms with partition rules that are similar to the one used here. The convergence proof given below is in the same spirit of the one given by Sherali and Alameddine.

Property S. The algorithm will either terminate in a finite number of partitions at a global optimal solution, or generate a sequence of bounds that converge to the global solution.

Proof Given the branch and bound procedure, there are two possibilities. In the first one, at a given node the lower bound C_L of the underestimator NLP_L is identical to the original objective function In which case the algorithm terminates in a finite number of partitions.

In the second possibility an infinite sequence of partitions is generated. This in turn implies that there is a subregion that is being infinitely partitioned. Let the sequence of solutions be denoted by $(^k)$ and $z=[Q, A, AT, x]$. By the termination criteria it is known that,

$$C^{u,k} - C_L^k > 0 \quad (38)$$

Since the upper bound is at least as strong as the evaluation of the actual objective function for the current solution z^k ,

$$C(z^k) - C(z^*) \geq C^{u,*} - C_L^{k^*} > 0 \quad (39)$$

there must exist an exchanger, m , for which its feasible region is infinitely partitioned. By the partition rule 1,

$$\left(\frac{Q}{\Delta T_1} - A_j\right) \leq \left(\frac{S}{\Delta T_m} - eA_m\right) \dots n \quad (40)$$

Summing up over all the exchangers i , it follows that.

$$n\left(\frac{Q_m}{\Delta T_m} - A_m\right) \geq C(z^k) - C_L(z^k) \geq C^{u,k} - C_L^k > 0 \quad (41)$$

The variables for exchanger m have some bounds defining an interval. Since the partition is of the same nature that the one used by Al-Khayyal and Falk, the variables in the sequence must converge to one of the bounds. Moreover, the series has to converge to a point since when one of the bounds of a variable are not changing this one is selected as the partition variable in the algorithm. When one of the variables is at the boundary the representation is exact - $\hat{A} = A_m$. Therefore,

which means that equality between the lower bound C_L and the original cost function C must hold. Since by Property 4 $C_L^{k^*}$ is a lower bound to the global optimal solution, it corresponds to the global solution.

Examples

In this section several examples are presented that illustrate the performance of the algorithm. The size and computational results of the examples are summarized in Table 2. The NLP time is the time used for solving the NLP_L problems and the LP time is the time for solving linear problems to obtain the initial bounds and subsequent updates. Note that in three of the examples only 1 node was required, which means that the problem was solved with the underestimator NLP_L without requiring branch and bound enumeration. These problems were solved with MINOS 5.2 using the modeling language GAMS on a IBM/R6000-530. Note that all the examples required less than 10 seconds of CPU-time. Moreover, the time for solving the LP bounding problems can be further reduced by using a warm start

Example 1

Consider the motivating example introduced earlier in this paper. If bounds are first computed for the variables, this yields the values shown in Table 3. The solution that had the lowest cost among these calculations has a cost of $C^* = \$36,160$ and the areas (A_i/U_i) are shown in Table 4 as the incumbent solution. The initial NLP_L is constructed using the nonlinear and linear estimator functions. In this example it is possible to obtain projections for the upper bound of the driving force over its heat load for exchangers 3 and 4 that can be used to generate underestimators of the form (24). These projections are given by:

$$AT_3 \leq 210 - 2Q_3 \quad (43)$$

$$AT_4 \leq 360 - 3Q_4 \quad (44)$$

The importance of these projections is that they provide an exact approximation for exchangers 3 and 4 as it can be seen by the solution of the first NLP_L in Table 4. The solution is $C_L^\circ = \$32,300$.

The actual objective function and the objective function of the convex NLP_L are plotted versus Q_i in Fig. 7. Since there is a gap between the Incumbent solution C^* and C_L° , a partition

is made. The largest difference in the approximations corresponds to exchanger 1. Since the incumbent solution lies at an extreme point it cannot be used to partition the space. Instead the convex solution is used to generate two subregions ($A_2 > 2.7 \text{ m}^2$ and $A^1 < 2.7 \text{ m}^2$ for Q^1 and Q^2 , respectively). For each one of these subregions the bounds on Q_2 and AT_2 are recalculated taking into account the **partition** constraint. The solutions of these **two new convex problems** are $C_L^1 = \$39,360$ and $C_L^2 = \$36,070$ C_L^1 . The first is greater than the incumbent solution ($C^{\#} = \$36,160$) so no further partition of this subregion is required. For the second subregion the lower bound is below the incumbent solution (0.2%) and a new partition is done similar to the first one. The only difference is that now the second exchanger is selected for partition. The solutions of the new subregions are $C_L^3 = \$36,270$ ($A^1 < 7.30 \text{ m}^2$) and $C_L^4 = \$36,160$ ($A^* \leq 7.30 \text{ m}^2$). The first of these subregions can be rejected while the first is equal to the incumbent solution, and therefore the global solution with $A^1 = 7.35$, $A_2 = 0.424$, $A_3 = 0.011$, $A_4 = 1.469 \text{ m}^2$ and $C = \$36,160$ has been obtained. The approximations of the objective function in the different subregions can be seen In Fig.8. The problem required a total of 4.1 sec. to find the global optimal solution as seen in Table 2.

Example 2

The same network as in example 1 is considered with the data given in Table 5 with $q = 1000 \text{ \$/m}^2$ and the overall heat transfer coefficients are $U_1 = U_2 = 0.1 \text{ KW}^r/\text{Km}^2$ and $U_3 = U_4 = 1.5 \text{ kW/K m}^2$. In this case there are two local minima and their objective function are close ($C = \$19,520$ and $C = \$19,160$). The algorithm obtains a tight lower bound In the first iteration ($O = \$18,640$) and behaves in a similar fashion as In the first example. The global optimum with $A_t = 9.647$, $A_a = 7.75$, $A_s = 0.577$, $A_4 = 1.188 \text{ m}^2$ and $O = \$1,9160$ is obtained after the solution of S NLP underestimator problems (see Table 2).

Example 3

The relevance of the projected underestimators (24) is illustrated by the following example. Consider the problem in Fig. 9. It consists of a cold stream that goes through two heat

exchangers In series. For the two hot streams the Inlet temperature are given and the outlet temperatures are not specified (see Fig 9).

In this case the cost function is given by the total area and the formulation is given by:

$$\min A = \frac{Q_1}{0.1 \Delta T_1} + \frac{Q_2}{0.1 \Delta T_2}$$

$$SL \quad \Delta T_1 = \frac{150 - T + T_1}{2}$$

$$\Delta T_2 = \frac{100 - T_1 + T_2}{2}$$

(p3)

$$Q = T - 300$$

$$Q_1 = 450 - T_1$$

$$Q_2 = 400 - T$$

$$Q_2 = 500 - T_2$$

$$300 \leq T \leq 400, T_1 \leq 450, T_2 \leq 500$$

$$Q_1, Q_2, \Delta T_1, \Delta T_2, T_1, T_2 \geq 0$$

Although the formulation of this problem is nonconvex, there is only one optimal solution. Moreover, if the objective function is plotted versus the heat load of the first heat exchanger (Q1) it is a convex function (see Fig. 10a).

When the algorithm is applied only using the nonlinear underestimator and linear overestimator functions (1) to (4) to approximate the nonconvex terms, it is not possible to obtain an exact approximation of the convex objective of this problem which is shown in Fig. 10b. If projections are generated for the upper bound of the driving forces in terms of their heat loads (22), the following inequalities are obtained:

$$AT \leq 150 - Q_1 \tag{45}$$

$$AT_2 \leq 100 \tag{46}$$

In this way, from (24), a new underestimator function can be generated for the first exchanger:

$$A_1 \geq \frac{Q_1}{\Delta T_1} = \frac{Q_i}{150 - Q_i} + AT, \quad \text{---} \quad \frac{100}{150 - Q_i} \quad \begin{matrix} M_{71} \\ (47) \end{matrix}$$

Once this projected underestimator (47) is added to the NLP underestimator problem, an exact approximation is obtained. When the objective function of NLP_L° is plotted, it matches exactly the original function in Fig. 10(a). In this way the solution of the underestimator problem has a total area of $AL^\circ = 9.49 \text{ m}^2$ and it is possible to prove global optimality in one iteration, by simply evaluating the actual objective function of this feasible solution and obtaining an incumbent solution of $A^* = 9.49 \text{ m}^2$ with $A_1 = 2.34 \text{ m}^2$ and $A_2 = 7.15 \text{ m}^2$. As seen in Table 2, the solution of this problem only required 0.75 sec.

Example 4

This example consists of one cold stream and three hot streams in a network of three heat exchangers in series (Fig. 11). The data are given in Table 6. This network is similar to the one presented in example 2 with the difference that now the problem does not project in a convex form. The objective function is to minimize the cost where $C_r = 1000 \text{ \$/m}^2$ and $U_f = 1 \text{ kW/K m}^2$. The algorithm is applied and it is possible to generate two extra projected underestimators (24) with the projections

$$AT_1 \leq 150 - 0.1Q_1 \quad (48)$$

$$AT_2 \leq 200 - 0.1Q_2 \quad (49)$$

The solution of the first convex underestimator problem is $C = \$6,420$ and when the real objective function for this feasible solution is evaluated the incumbent solution is $C^\# = \$6,420$ and hence the global solution with $A_1 = 0 \text{ m}^2$, $A_2 = 1.54 \text{ m}^2$ and $A_3 = 4.88 \text{ m}^2$ is obtained in only one iteration. As seen in Table 2, this problem required 1.77 sec

Example 5

The same network as in the previous example is considered, with the new data given in Table 7. In this case the global solution is not an extreme point like in the previous one and the

approximations are not exact in the first iteration. The solution of this first convex problem is $C_L^\circ = \$6,269$ and the incumbent solution is $C^\# = \$6,482$. The approximations for the first and third heat exchangers are exact, so then the second heat exchanger is selected. Here the linear overestimator are redundant and the partitions are made over the heat load. Two subregions are obtained with the constraints $Q_2 \leq 26.8$ and $Q_2 \geq 26.8$ with convex solutions of $C_L^* = \$6,408$ and $C_L^2 = \$6,278$, respectively. The incumbent solution now is $C^* = \$6,408$ so the first subregion does not require more partitioning. For the remaining subregion a partition is made taking now the driving force of the second heat exchanger. The subregions are $AT_2 \leq 165.89$ and $AT_2 \geq 165.89$ with solutions $C^1 = \$6,355$ and $C_L^4 = \$6,373$ respectively. No better upper bound is obtained and since the lower and upper bound are close the original problem is solved given a new incumbent solution of $C^* = \$6,398$. The subregions are within a 0.6% of the incumbent solution, and the algorithm stops with $A^1 = 0.6253 \text{ m}^2$, $A_2 = 1.219 \text{ m}^2$ and $A_3 = 4.55 \text{ m}^2$. If a smaller ϵ is used ($\epsilon = 0.2\%$) four more NLP's are solved. Thus, with the larger tolerance 3.95 sees and 5 NLP's were required, while with the smaller tolerance 9 NLP's were required with 5.1 sees as seen in Table 2.

Example 6

The next example is the one presented by Colbeig and Morari (1990) and Yee *et al* (1990). Here a fixed configuration is considered and the network is shown in Fig. 12 and the objective is to minimize the area. Two local solutions are listed in Table 8. Applying the algorithm it is possible to generate projections for three of the seven heat exchangers. In the initial underestimator a lower bound of 242.78 m^2 is obtained. The actual objective function for this solution is 252.8 m^2 . The largest difference corresponds to the A_{cmi}^* and the level chosen for the partition is 24.696 . For $A_{cm} \leq 24.696$ the convex solution has an objective of $A = 246.39 \text{ m}^2$, and for the other subregion the solution is $A = 245.1 \text{ m}^2$. A better incumbent solution is obtained with an objective of $A = 245.6 \text{ m}^2$ and the solution is within 0.2% of the global solution. Only three convex NLP underestimator subproblems were required to converge in a total of 7.33 sees as seen in Table 2.

Example 7

The following example consists of a network reported In Grossmann and Floudas (1987). The configuration is illustrated in Fig. 13 and the data is given in Table 9. The objective function is to minimize the total area of the network and $U_t = 0.5 \text{ kW/K m}^2$.

For this problem it was possible to identify the following six projection terms:

$$A^{\wedge} \leq 89.5 - 0.022 Q_1$$

$$AT_2 \geq 89.5 - 0.022 Q_x$$

$$AT_4 \leq 46.24 - 0.008 Q_4 \quad (50)$$

$$AT_5 \leq 63.66 - 0.011 Q_5$$

$$AT_6 \leq 13 - 0.005 Q_6$$

$$\Delta T_6 \geq 13 - 0.005 Q_6$$

The solution of the first underestimator problem is $C_L^l = 537.966 \text{ m}^2$ and the evaluation of the original function has the same value. Therefore, the optimal solution with $A_i = 53.33 \text{ m}^2$, $A_a = 100 \text{ m}^2$, $A_b = 34.28 \text{ m}^2$, $A^* = 87.95 \text{ m}^2$, $A_s = 149.94 \text{ m}^2$, $A^{\wedge} = 52.17 \text{ m}^2$, $A_y = 26.66 \text{ m}^2$ and $A_e = 36.61 \text{ m}^2$ is obtained after 5.46 sees, (see Table 2).

Conclusions

*

This paper has presented a global optimization algorithm for heat exchanger networks that can be formulated In terms of linear rational functions In the objective function and linear constraints. The key element in the proposed algorithms are the proposed convex nonlinear underestimators for rational terms which complement the linear underestimators for bilinear terms by McCormick (1983). As has been shown with the numerical results, the resulting NLP underestimator problem provides rigorous tight lower bounds to the global optimum with which the computational effort in the spatial branch and bound method is greatly reduced. In

fact for all cases except one only a maximum of 5 nodes had to be enumerated in the example problems.

Finally, it should be noted that the method proposed in this paper has been generalized to nonlinear programs that involve convex, linear rational and bilinear terms in the objective function and constraints (Quesada and Grossmann, 1992). Also, work is under way to be able to handle concave cost functions and logarithmic mean temperature differences in the heat exchanger network, as well as the optimization of the configurations.

Acknowledgment

The authors would like to acknowledge financial support from the Engineering Design Research Center at Carnegie Mellon University.

Appendix A. Linear and nonlinear under and overestimators.

A concave overestimating function of a product of functions is given by (McCormick (1983)),

$$f(x)g(y) \leq \min[f^u C_g(y) + g^l C_f(x) - f^u g^l, f^l C_g(y) + g^u C_f(x) - f^l g^u] \quad (A1)$$

where $C_f(x)$ and $C_g(y)$ are concave functions such that for all x and y in some convex set:

$$C_f(x) \geq f(x) \quad (A2)$$

$$C_g(y) \geq g(y) \quad (A3)$$

Considering the function $A_i A_j$, where $f(x) = A_i$, and $g(x) = A_j$, the concave functions $C_f(x)$ and $C_g(y)$ are functions $f(x)$ and $g(y)$, respectively. The concave overestimating function, which is linear. Is given by:

$$A_i A_j \leq \min[A_i A_j, A_i A_j^u, A_i^u A_j, A_i A_j^l, A_i^l A_j] \quad (A4)$$

In a similar way as in (A1), the convex underestimating function of a product of functions is given by:

$$f(x)g(y) \geq \max[f^l C_g(y) + g^u C_f(x) - f^l g^u, f^u C_g(y) + g^l C_f(x) - f^u g^l] \quad (A5)$$

where F^l , G^u and G^l are positive bounds over the functions $f(x)$ and $g(y)$ such that

$$F^l \leq f(x) \leq F^u \quad (A6)$$

$$G^l \leq g(y) \leq G^u \quad (A7)$$

and $q(x)$ and $C_g(y)$ are convex functions such that for all x and y in some convex set:

$$q(x) \leq C_q(x) \quad (A8)$$

$$C_g(y) \leq g(y) \quad (A9)$$

Based on (A51) one can generate nonlinear underestimators for the rational terms in the objective function of problem (P) as follows. In particular, consider the function $\frac{Q_i}{\Delta T_i}$, where $f(x) = Q$, and $g(y) = \frac{1}{\Delta T}$. The functions and bounds are given by:

$$c_f(x) = Q_i \tag{A10}$$

$$c_g(y) = \frac{1}{\Delta T_i} \tag{A11}$$

$$Q^L \leq Q_i \leq Q^U \tag{A12}$$

$$\frac{1}{\Delta T_i^U} \leq \frac{1}{\Delta T_i} \leq \frac{1}{\Delta T_i^L} \tag{A13}$$

From (A51) the convex underestimator function is given by:

$$\frac{Q}{\Delta T_i} \geq \max \left[\frac{Q}{\Delta T_i^U} + Q^L \left(\frac{1}{\Delta T_i} - \frac{1}{\Delta T_i^U} \right), \frac{Q}{\Delta T_i^L} + Q^U \left(\frac{1}{\Delta T_i} - \frac{1}{\Delta T_i^L} \right) \right] \tag{A14}$$

Appendix B. On the exact approximation of the linear and nonlinear estimators in the boundary.

The estimator functions (A4) and (A14) have the property that they match the function when one of the variables is at a bound. This is because the individual convex and concave approximation functions in (A2), (A3), (A8) and (A9) are the functions themselves.

Equation (A4) for the linear overestimator reduces as follows:

if $A_i = A_i^U$

$$A_i^U \Delta T_i \leq \min [A_i^L \Delta T_i + A_i^U \Delta T_i - A_i^L \Delta T_i, A_i^U \Delta T_i + (A_i^U - A_i^L) \Delta T_i] = A_i^U \Delta T_i \tag{B1}$$

if $A_i = A_i^L$

$$A_i^L \Delta T_i \leq \min [A_i^L \Delta T_i + (A_i^U - A_i^L) \Delta T_i, A_i^L \Delta T_i] = A_i^L \Delta T_i \tag{B2}$$

if $\Delta T_i = \Delta T_i^U$

$$A_i \Delta T_i^U \leq \min [A_i \Delta T_i^U, A_i \Delta T_i^U + (A_i^U - A_i) \Delta T_i^U] = A_i \Delta T_i^U \tag{B3}$$

if $\Delta T_i = \Delta T_i^L$

$$A_i \Delta T_i^L \leq \min [A_i \Delta T_i^L, (A_i - A_i^L) \Delta T_i^L + A_i \Delta T_i^L] = A_i \Delta T_i^L \tag{B4}$$

Equation (A14) for the convex nonlinear underestimator reduces as follows:

if $\Delta T_j = \Delta T_i^U$

$$\begin{aligned} \frac{Q}{\Delta T_i^U} &\geq \max \left[\frac{Q}{\Delta T_i^U}, \frac{Q}{\Delta T_i^L} + Q^U \left(\frac{1}{\Delta T_i^U} - \frac{1}{\Delta T_i^L} \right) \right] = \max \left[\frac{Q}{\Delta T_i^U}, \frac{Q}{\Delta T_i^L} + \frac{Q}{\Delta T_i^U} - \frac{Q}{\Delta T_i^L} + Q^U \left(\frac{1}{\Delta T_i^U} - \frac{1}{\Delta T_i^L} \right) \right] \\ &= \max \left[\frac{Q}{\Delta T_i^U}, \frac{Q}{\Delta T_i^U} + (Q^U - Q) \left(\frac{1}{\Delta T_i^U} - \frac{1}{\Delta T_i^L} \right) \right] = \frac{Q}{\Delta T_i^U} \end{aligned} \quad (B5)$$

similarly when $\Delta T_i = \Delta T_i^L$

$$\frac{Q}{\Delta T_i^L} \geq \max \left[\frac{Q}{\Delta T_i^U} + Q^L \left(\frac{1}{\Delta T_i^L} - \frac{1}{\Delta T_i^U} \right), \frac{Q}{\Delta T_i^L} \right] = \max \left[\frac{Q}{\Delta T_i^L} + (Q^L - Q) \left(\frac{1}{\Delta T_i^L} - \frac{1}{\Delta T_i^U} \right), \frac{Q}{\Delta T_i^L} \right] = \frac{Q}{\Delta T_i^L} \quad (B6)$$

for $Q_i = Q_i^U$

$$\frac{Q^U}{\Delta T_i} \geq \max \left[\frac{Q^U}{\Delta T_i^U} + (Q^U - Q_i) \left(\frac{1}{\Delta T_i} - \frac{1}{\Delta T_i^U} \right), \frac{Q^U}{\Delta T_i^L} \right] = \max \left[\frac{Q^U}{\Delta T_i} + (Q^U - Q_i) \left(\frac{1}{\Delta T_i} - \frac{1}{\Delta T_i^U} \right), \frac{Q^U}{\Delta T_i^L} \right] = \frac{Q^U}{\Delta T_i} \quad (B7)$$

finally for $Q_j = Q_i^L$

$$\frac{Q^L}{\Delta T_i} \geq \max \left[\frac{Q^L}{\Delta T_i}, \frac{Q^L}{\Delta T_i^L} + Q^U \left(\frac{1}{\Delta T_i} - \frac{1}{\Delta T_i^L} \right) \right] = \max \left[\frac{Q^L}{\Delta T_i}, \frac{Q^L}{\Delta T_i} + (Q^U - Q^L) \left(\frac{1}{\Delta T_i} - \frac{1}{\Delta T_i^L} \right) \right] = \frac{Q^L}{\Delta T_i} \quad (B8)$$

References

- Al-Khayyal, F.A. and Falk, J.E. (1983) Jointly constrained biconvex programming. *Mathematics of Operations Research* 8, 273-286
- Charnes, A. and Cooper. W.W. (1962) Programming with linear **fractional functionals**. *Naval Research Logistics Quarterly* 9, 181-186
- Colberg, R.D. and Morari, M. (1990) Area and capital cost targets for heat exchanger network synthesis **with constrained matches and unequal** heat transfer coefficients. *Computes chem. Engng.* 14, 1-22
- Dinkelbach, W. (1967) **On** nonlinear fractional programming. *Management Science* 13, 492-498
- Dolan, W.B., Cummings, P.T. and LeVan, M.D. (1989) **Process optimization via simulated annealing: application to network design**, *AIChE Journal* 35 ,725-736
- Falk, J.E. and Palocsay, S.W. (1991) **Optimizing the sum of linear fractional functions**. *Recent Advances in Global Optimization*. Edited by Floudas, C.A and Pardalos, P.M., 221-258
- Floudas, C.A., Cirtc, A.R. and Grossmann, I.E. (1986) Automatic synthesis of optimum heat exchanger network configurations. *AIChE Journal* 32, 276-290
- Floudas, CA. and Visweswaran, V., (1990) A global optimization algorithm (GOP) for certain classes of nonconvex NLPs-I Theory, *Computes chem. Engng.* 14, 1397-1417
- Floudas, CA. and Visweswaran, V. (1990) A global optimization algorithm (GOP) for certain classes of nonconvex NLPs-n Application of theory and test problems. *Computes chem. Engng.* 14,1418-
- Grossmann, I.E, and Floudas, CA. (1987) Active constraint strategy for flexibility analysis in chemical process. *Computes chem. Engng.* 11,675-693
- Gundersen, T. and Naess, L. (1988) The synthesis of cost optimal heat exchanger network synthesis- an industrial review of the state of the art *Computers chem. Engng* 12, 503-530
- Horst, R (1990) Deterministic method in constrained global optimization: Some recent advances and fields of application. *Naval Research Logistics.* 37,433-471
- McConnick, G.P. (1983) *Nonlinear Programming*. John Wiley & Sons

Quesada, I. and Grossmann, I.E. (1992). Global optimization algorithm for rational and bilinear programs. Manuscript in preparation.

Sherali, H.D. and Alameddine, A. (1990) A new reformulation-linearization technique for bilinear programming problems, presented at ORSA/TIMS meeting Philadelphia

Swaney, R.E. (1990) Global solution of algebraic nonlinear programs. Paper No.22f presented at AIChE Meeting , Chicago, IL

Westerberg, A.W. and Shah, J.V. (1978) Assuring a global optimum by the use of an upper bound on the lower (dual) bound. *Computers them. Engng* 2, 83-92

Yee, T.F., Grossmann, I.E. and Kravanja, Z. (1990) Simultaneous optimization models for heat integration-L Area and energy targeting and modeling of multi-stream exchangers. *Computers cherthEngng* 14,1151-1164

Yee, T.F., and Grossmann, I.E. (1990) Simultaneous optimization models for heat integration-n. Heat exchanger network synthesis. *Computers chem. Engng* 14, 1165-1184

Table 1. Data for motivating example.

Streams	Fcp (kW/K)	Temperature	
		Inlet (K)	Outlet (K)
C1	1	300	400
C2	5.55	365	—
C3	3.57	358	—
H1	4.54	575	395
H2	3.125	718	398

Table 2. Size and computational results of example problems.

Problem	Size ¹		Initial objective		Global optimum	No. of nodes	LP time ²	NLP time ²
	Original	NLP _T	C _T	C*				
Ex1	(12.13)	(16.31)	32 [^] 00	36.160	36.160	5	3.20	0.90
Ex 2	(12.13)	(16.31)	18.640	19.160	19.160	5	3.20	1.05
Ex 3	(7.6)	(9.11)	9.49	9.49	9.49	1	0.65	0.10
Ex 4	(11.9)	(14.23)	6.420	6.420	6.420	1	1.50	0.22
Ex 5	(11.9)	(14.23)	6.269	6.482	6 [^] 98	5	2.70	1.25
(e=0.2%)						(9)	(3.90)	(2.20)
Ex 6	(20.21)	(27.52)	242.78	252.8	245.5	3	5.23	2.10
EJC7	(26.30)	(27.68)	537.97	537.97	537.97	1	5.03	0.43

¹ (m, n)_T m = # of variables, n = # of constraints

² CPU seconds in a IBM/R6000-530

Table 3. Initial lower and upper bounds for example 1.

Heat Exchanger	LBArea (m ²)	UBArea (m ²)	LB Heat Load (KW)	UBHeat Load(kW)	LB AT (K)	UB AT (K)
1	1.11	7352	5.55	973125	50	133.03
2	0.425	4.743	2.1875	94.44	51.5	199.11
3	0.0106	4.474	2.1875	94.44	21.11	205.625
4	0.0162	1.469	5.55	97.8125	66.5625	34333

Table 4. Area for first convex underestimator In example 1.

Heat Exchanger	Convex Solution	Exact Solution	Incumbent Solution
1	5.95	6.74	7.35
2	1.46	2.70	0.424
3	0.14	0.14	0.0106
4	0.60	0.60	1.469

Table 5. Data for example 2.

Streams	Fcp (kW/K)	Temperature	
		Inlet (K)	Outlet (K)
C1	1	250	400
C2	1	370	—
C3	1	352.5	—
H1	1	580	380
H2	1	512.5	362.5

Table 6. Data for example 4.

stream	Temperature (K)		Fcp (kW/K)
	Inlet	Outlet	
C1	300	400	10
H1	450	—	10
H2	500	—	10
H3	550	—	10

Table 7. Data for example 5.

stream	Temperature (K)		Fcp (KW/K)
	Inlet	Outlet	
C1	300	400	10
H1	490	...	10
H2	500	...	10
H3	550	—	10

Table 8. Areas for local solutions in example 5.

stream	A_{H1C1}	A_{H2C1}	A_{H2C2}	A_{C1}	A_{C2}	A_{H1}	A_{H2}	Total
1	38.27	325.11	73.13	6.55	4.15	1.59	42.76	491.61
2	30.53	45.41	107.9	6.70	2.74	0.00	52.34	245.62

Table 9. Data for example 7.

Stream	Pcp	Inlet T	Outlet T
H1	40	400	325
H2	20	450	350
H3	20	400	360
H	—	540	530
C1	50	310	380
C2	60	290	410
C3	20	285	340

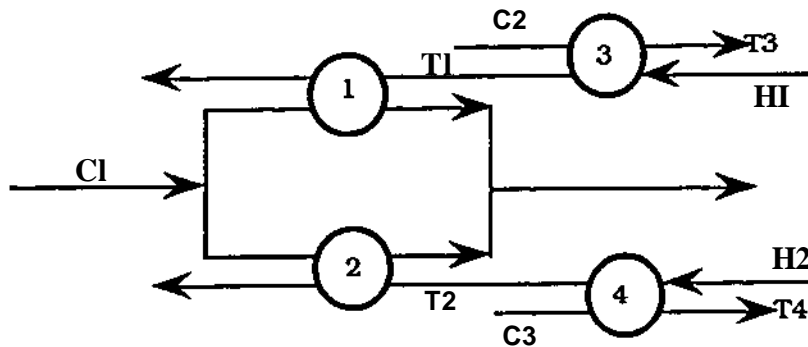


Figure 1. Network for motivating example.

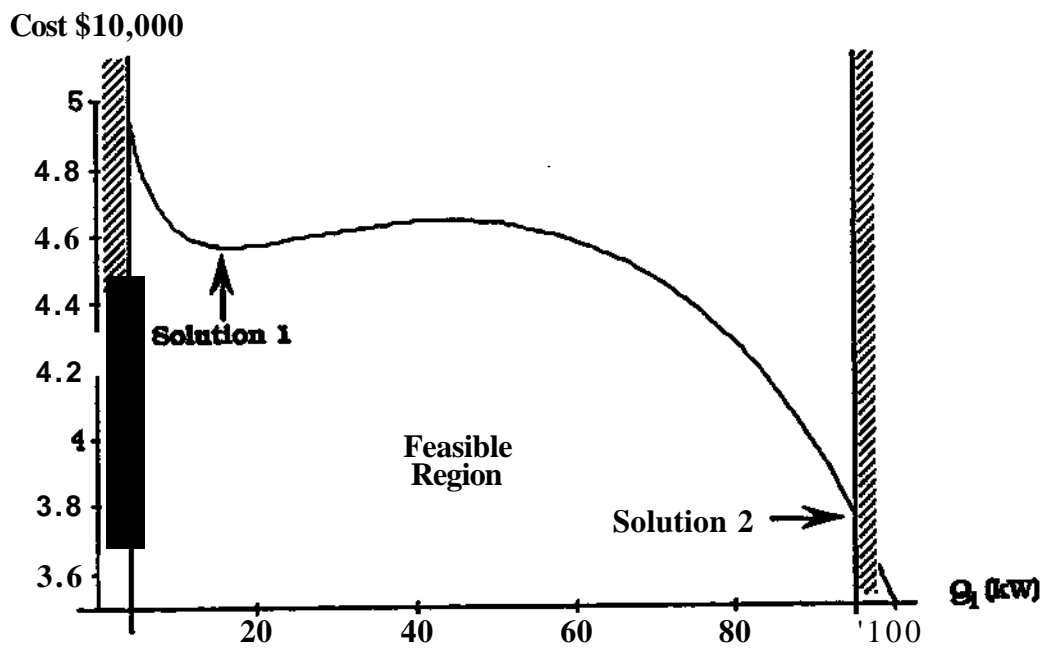


Figure 2. Cost of the network versus Q_1 for the motivating example.

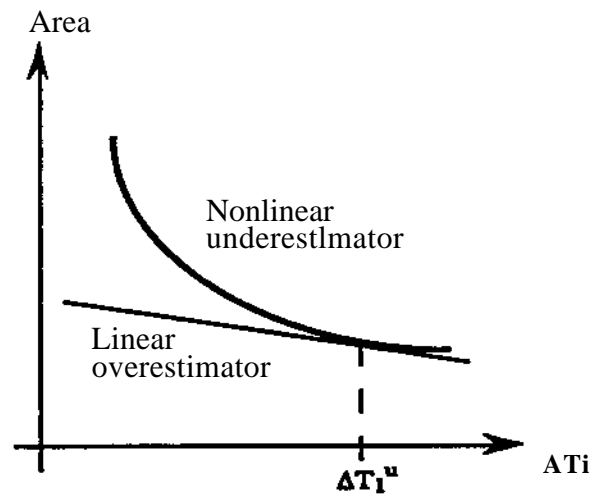


Figure 3. Comparison between nonlinear and linear estimators.

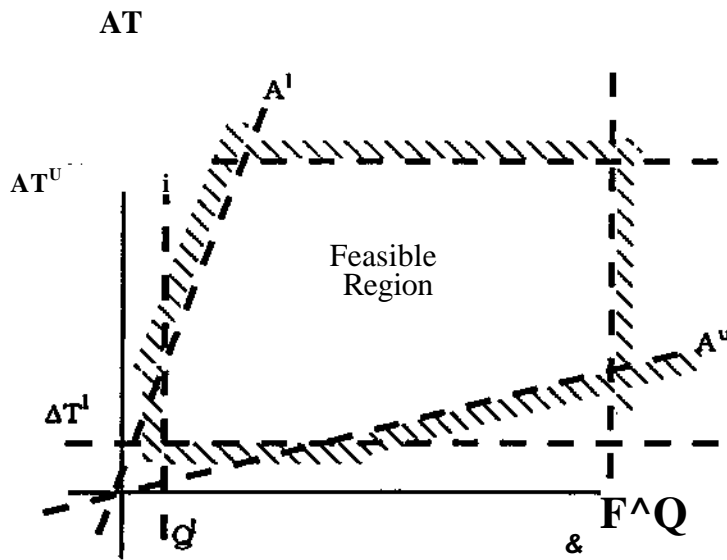


Figure 4. Feasible region in space Q - AT for a given exchanger.

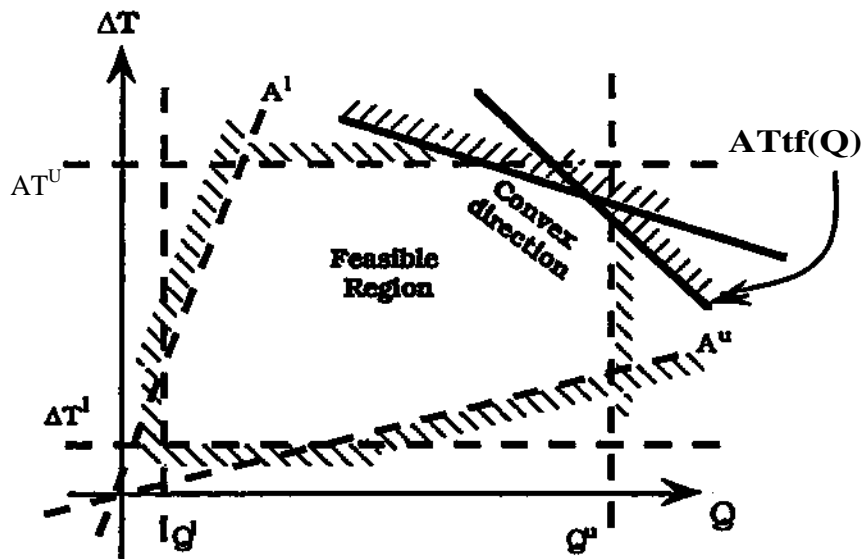


Figure 5. Convex directions in the feasible region for the fractional terms.

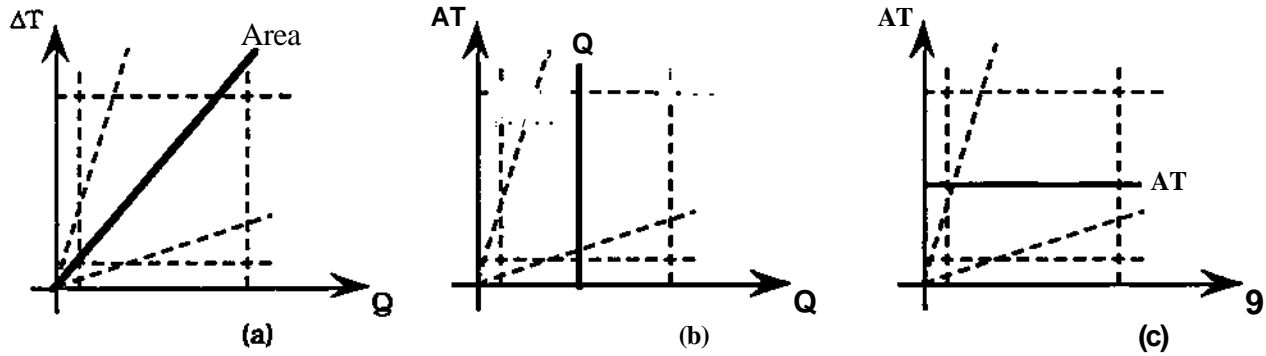


Figure 6. Partitions of the feasible region for (a) Area, (b) Heat load and (c) Driving force.

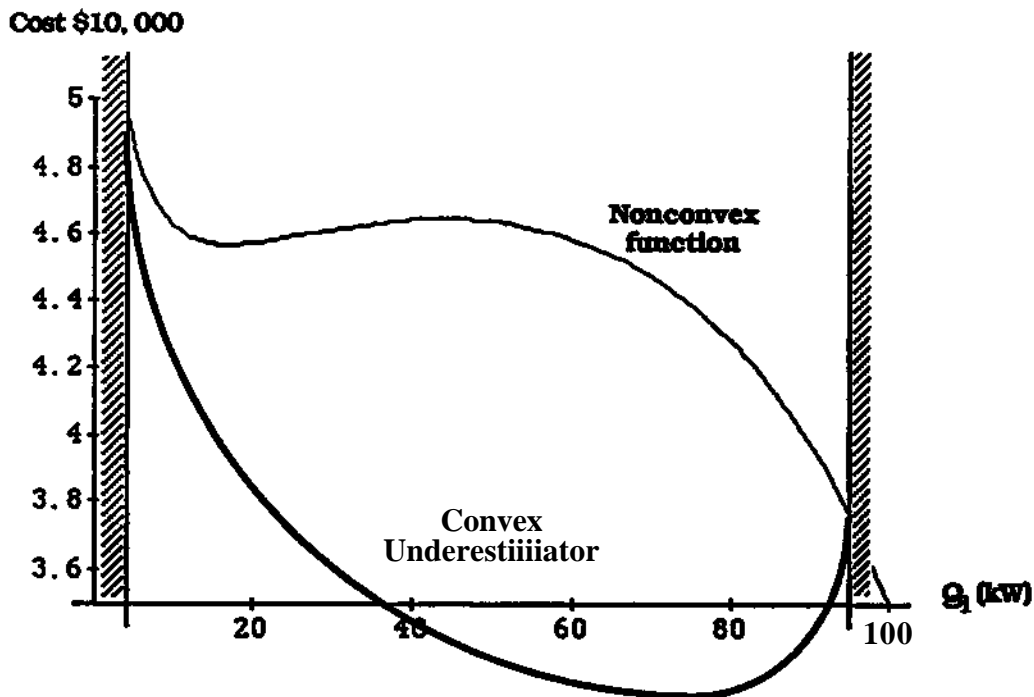


Figure 7. Plot of first convex underestimator In example 1.

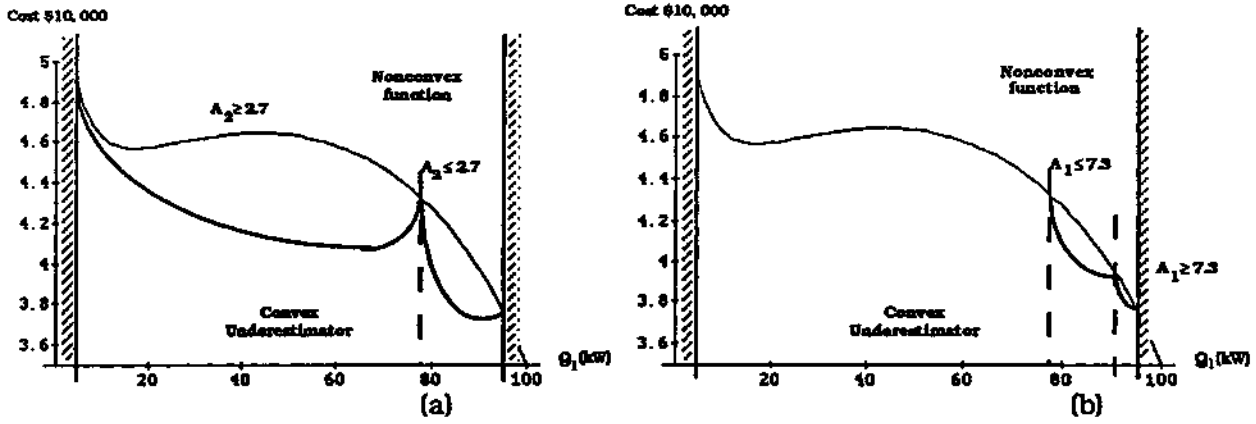


Figure 8. Partitions for example 1 (a) First partition, (b) Second partition.

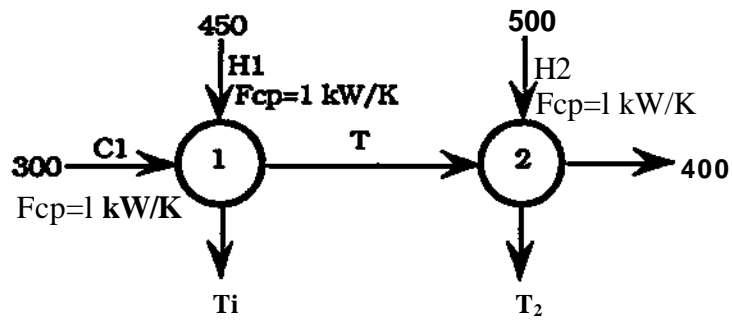


Figure 9. Network for example 3.

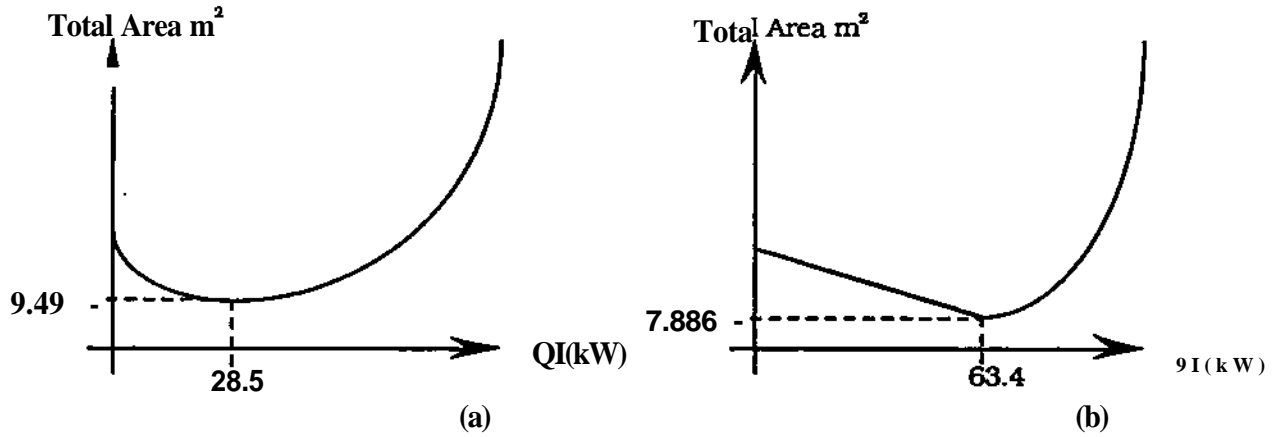


Figure 10. (a) Original objective function for example 3. (b) Objective with linear and nonlinear underestimators.

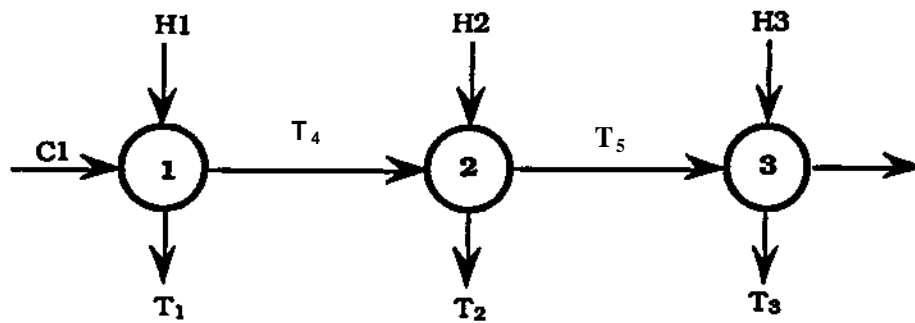


Figure 11. Network for example 4.

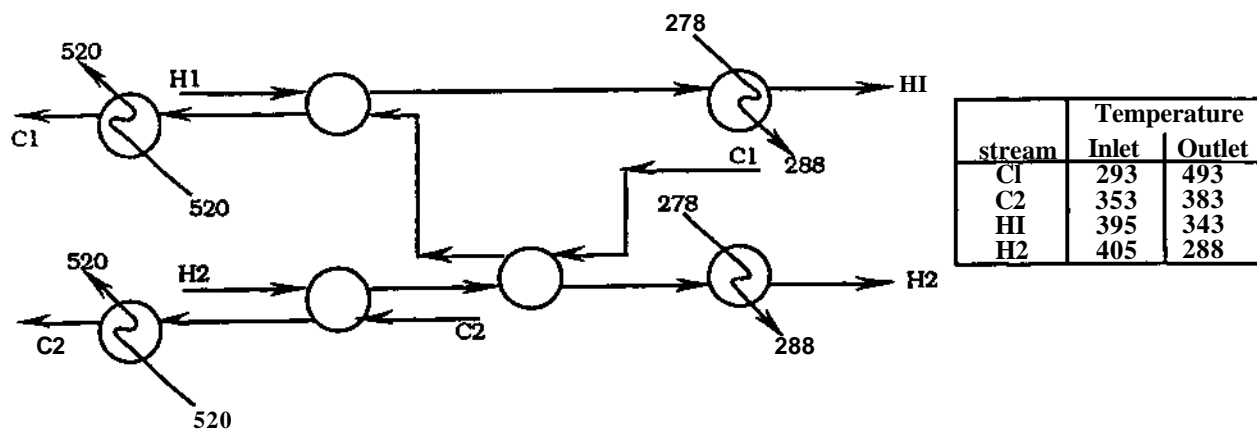


Figure 12. Network for example 6.

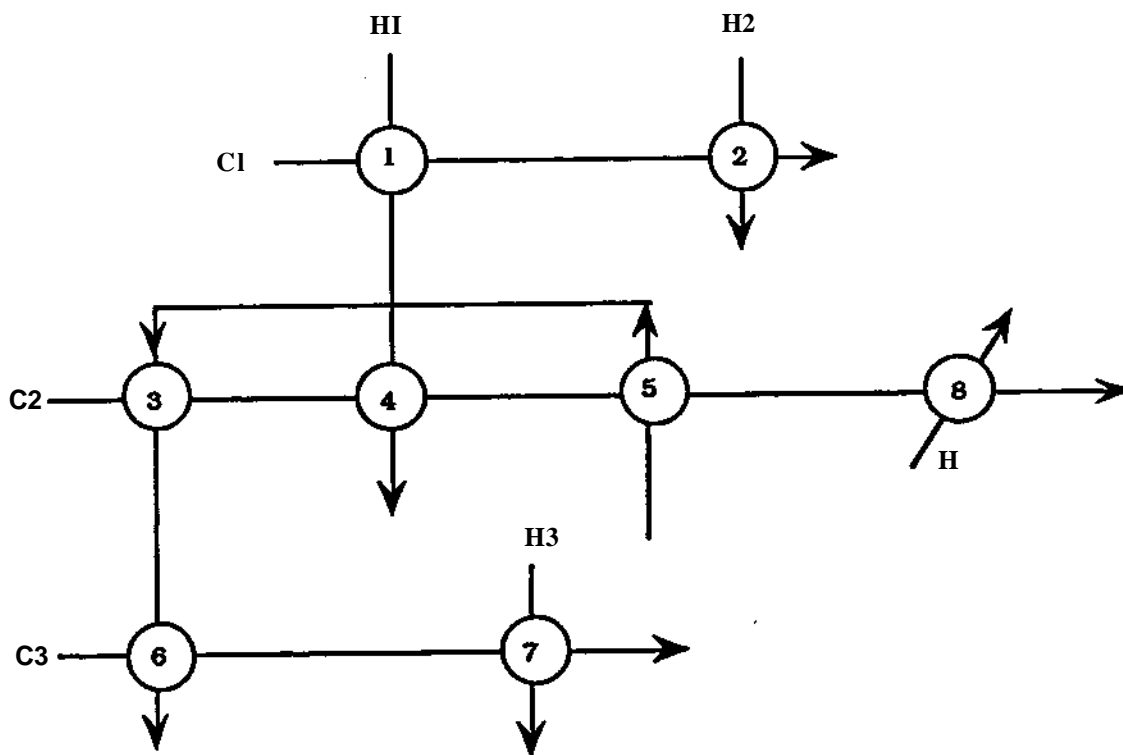


Figure 13* Network for example 7.